Original Article

Diagnostic value of computed tomography myocardial perfusion imaging to detect coexisting microvascular dysfunction in patients with obstructive epicardial coronary artery disease

Masahiro Hada[1]^, Masahiro Hoshino[1], Tomoyo Sugiyama[2], Yoshihisa Kanaji[1], Eisuke Usui[1], Yoshihiro Hanyu[1], Tatsuhiro Nagamine[1], Kai Nogami[1], Hiroki Ueno[1], Kazuki Matsuda[1], Tatsuya Sakamoto[1], Taishi Yonetsu[2], Tetsuo Sasano[2], Tsunekazu Kakuta[1]

[1]Division of Cardiovascular Medicine, Tsuchiura Kyodo General Hospital, Ibaraki Prefecture, Japan; [2]Department of Cardiovascular Medicine, Tokyo Medical and Dental University, Tokyo, Japan

Contributions: (I) Conception and design: M Hoshino, T Kakuta; (II) Administrative support: T Kakuta; (III) Provision of study materials or patients: M Hada, M Hoshino, T Sugiyama, E Usui, Y Hanyu, T Nagamine, K Nogami, H Ueno, K Matsuda, T Sakamoto; (IV) Collection and assembly of data: M Hada, K Matsuda; (V) Data analysis and interpretation: M Hada, M Hoshino, T Kakuta; (VI) Manuscript writing: All authors; (VII) Final approval of manuscript: All authors.

Correspondence to: Tsunekazu Kakuta, MD, PhD. Division of Cardiovascular Medicine, Tsuchiura Kyodo General Hospital, 4-1-1, Ohtsuno, Tsuchiura City, Ibaraki Prefecture, Japan. Email: kaz@joy.email.ne.jp.

Background: Computed tomography myocardial perfusion (CT-MP) has reported usefulness in assessing hemodynamically significant epicardial coronary artery lesions. However, the diagnostic ability of the absolute coronary flow using CT-MP to detect coronary microvascular dysfunction (CMD) remains elusive. This prospective cohort study aimed to assess the diagnostic value of CT-MP in evaluating coexisting CMD in patients with functionally significant epicardial coronary stenosis and to analyze the predictive factors of lesions with CMD.

Methods: Sixty-eight patients with chronic coronary syndrome (CCS) and *de novo* single functionally significant stenosis [fractional flow reserve (FFR) ≤0.80] were studied. CMD was defined as an index of microcirculatory resistance ≥25. We compare clinical background and CT-MP findings between patients with and without CMD (CMD, n=29; non-CMD, n=39). CT-MP, and quantitative and qualitative plaque assessments were included in computed tomography angiography assessment. Logistic regression analysis was performed to predict CMD.

Results: FFR, invasive wire-derived coronary flow reserve (CFR_{wire}) and index of microcirculatory resistance were 0.68 [interquartile range (IQR), 0.59–0.74], 1.71 (IQR, 1.24–2.88), and 22.6 (IQR, 15.1–34.5), respectively. The rest and hyperemic-myocardial blood flow (MBF) and CT-MP-derived CFR ($CFR_{CT\text{-}MP}$) were 0.83 (0.64–1.03) mL/min/g, 2.14 (1.30–2.92) mL/min/g, and 2.19 (1.44–3.37), respectively. In the territories with CMD, hyperemic-MBF was significantly lower than in those without [1.68 (IQR, 0.84–2.44) *vs.* 2.31 (IQR, 1.67–3.34) mL/min/g, P=0.015] and the prevalence of $CFR_{CT\text{-}MP}$ <2.0 was higher in the lesions with CMD than in those without (62.1% *vs.* 28.2%, P=0.011), while FFR values were similar. Fibrofatty and necrotic core component volume was greater in the vessels with CMD than in those without [31.8 (IQR, 19.0–48.9) *vs.* 25.1 (IQR, 17.2–32.1) mm^3, P=0.045]. Multivariable logistic regression analysis showed that hyperemic-MBF and fibrofatty and necrotic core component volume were independent predictors of CMD territories [odds ratio (OR) =0.583; 95% confidence interval (CI): 0.355–0.958; P=0.033 and OR =1.040; 95% CI: 1.010–1.070; P=0.011].

^ ORCID: 0000-0003-1499-9188.

Conclusions: Quantitative assessment of absolute coronary flow using pre-percutaneous coronary intervention (PCI) CT-MP, and comprehensive plaque analysis using computed tomography angiography may help detect coexisting subtended microvascular dysfunction in territories with functionally significant epicardial coronary lesions. Further studies are required to elucidate the clinical significance of coexisting CMD in patients with CCS undergoing PCI.

Keywords: Coronary microvascular dysfunction (CMD); computed tomography myocardial perfusion (CT-MP); chronic coronary syndrome (CCS)

Submitted May 06, 2023. Accepted for publication Oct 07, 2023. Published online Nov 21, 2023.
doi: 10.21037/qims-23-618
View this article at: https://dx.doi.org/10.21037/qims-23-618

Introduction

The efficacy of computed tomography myocardial perfusion (CT-MP) in detecting ischemic regions has been repeatedly reported (1,2). A significant correlation has been reported between absolute myocardial blood flow (MBF) calculated using dynamic CT-MP and ^{15}O-HsO positron-emission tomography in patients with coronary artery disease (3). Recently, coronary microvascular dysfunction (CMD) has been increasingly evaluated as a significant factor in the signs and symptoms of myocardial ischemia (4). Presence of CMD and diabetes were reported to be independent predictors of major adverse cardiovascular events in the 2-year follow-up period after fractional flow reserve (FFR)-guided revascularization (5). Myocardial ischemia caused by CMD has prognostic value for patients with chronic coronary syndrome (CCS) (6). We previously reported that CMD is associated with fibrofatty and necrotic component (FFNC) volume and epicardial fat volume on coronary computed tomography (CT) analysis (7). However, limited data are available regarding the prevalence of coexisting CMD in patients undergoing percutaneous coronary intervention (PCI) and the impact of CMD on absolute coronary flow. Therefore, the present study sought to (I) investigate the diagnostic value of coronary computed tomography angiography (CCTA) and quantitative evaluation of absolute coronary flow by CT-MP to detect coexisting CMD in patients with significant epicardial coronary stenosis and (II) analyze the predictive factors for territories with CMD before PCI. We present this article in accordance with the STROBE reporting checklist (available at https://qims.amegroups.com/article/view/10.21037/qims-23-618/rc).

Methods

Study design and patient population

Consecutive patients scheduled for elective PCI with anginal symptoms (Canadian Cardiovascular Society class 1–3) after physiological proof of ischemia by FFR in diagnostic coronary angiography were prospectively recruited from a single tertiary care center between April 2019 and November 2021. All patients had functionally significant *de novo* stenotic lesions in a single coronary artery (positive noninvasive test results or invasive tests, including FFR ≤0.80, or positive resting indices). Acute coronary syndrome patients were excluded. Patients with the inability to provide consent, history of myocardial infarction, occluded target vessels, left main coronary artery disease, chronic renal disease, and contraindications to adenosine were excluded. Of the 97 initially enrolled patients who underwent CT-MP before the scheduled PCI, 29 were excluded due to insufficient CT imaging for plaque analysis, CT-MP data acquisition, or incomplete physiological data. Thus, 68 patients who underwent a successful PCI and had complete CT-MP data were finally analyzed (*Figure 1*). Optimal medical therapy including high-dose statins, dual antiplatelets, and antihypertensives was administrated immediately after diagnostic catheterization in all enrolled patients. *Ad hoc* PCI was not performed in the study patients according to the study protocol.

The study was approved by the Institutional Ethics Committee of Tsuchiura Kyodo General Hospital (reference #808/Tsuchiura; March 22, 2019) and conducted in compliance with the tenets of the Declaration of Helsinki (as revised in 2013) for investigations with human participants.

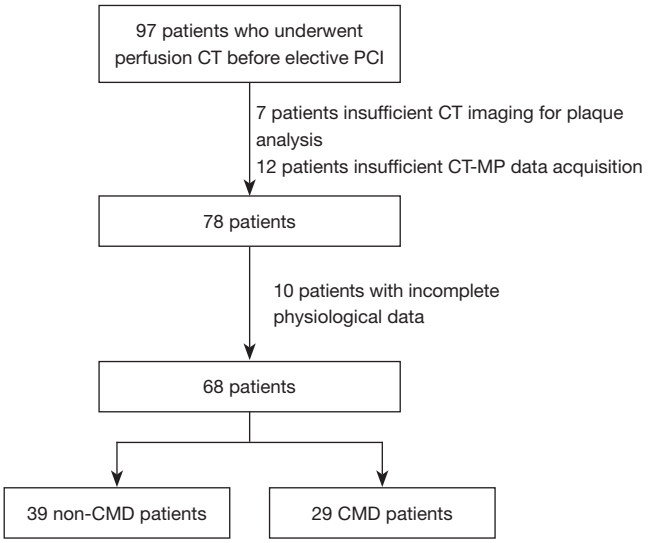

Figure 1 Flow diagram of included patients. CT, computed tomography; PCI, percutaneous coronary intervention; CT-MP, computed tomography myocardial perfusion; CMD, coronary microvascular dysfunction.

Written informed consent for the study and future data use for retrospective analyses was provided by all patients.

Invasive coronary angiography, PCI, and FFR measurements

Standard diagnostic coronary angiography was initially performed via the radial artery using a 5F system to assess the coronary anatomy and severity of functional stenosis. Quantitative coronary angiography analysis was performed using the CMS-MEDIS system (Medis Medical Imaging Systems, Leiden, The Netherlands). A bolus heparin (5,000 IU) is injected before the angiography. Intracoronary nitroglycerin (0.2 mg) administration was performed at the start of the procedure and before functional measurements.

The FFR, mean transit time (Tmn), coronary flow reserve (CFR) and index of microcirculatory resistance (IMR) values were determined using a Radi Analyzer Xpress instrument with a single 0.014-inch PressureWire^{TM} (Abbott Vascular, St. Paul, MN, USA) at the time of diagnostic catheterization or before PCI. The FFR value was calculated as the ratio of the mean distal coronary pressure to the mean aortic pressure during stable hyperemia, which was induced by intravenous adenosine (140 μg/kg/min through a central vein). At first, the pressure guidewire was calibrated at the tip of guiding catheter. And then, the wire was advanced distal to the coronary stenosis, and the intracoronary pressure was measured. Subsequently, 3 mL of room-temperature saline was administrated three times, and the baseline Tmn was determined. CFR was defined as the resting Tmn divided by the hyperemic Tmn. The IMR was calculated as follows: $IMR = P_a \times T_{mn}\ [(P_d - P_w)/(P_a - P_w)]$, where P_a is the aortic pressure during maximum hyperemia, P_d is the distal coronary pressure during maximum hyperemia, and P_w is the coronary wedge pressure (8). CMD was defined by IMR ≥25. Strict prohibition of ingesting caffeinated beverages was instructed for >24 hours before catheterization. Eligible patients who had non-totally occluded and functionally significant stenosis (FFR ≤0.80) subsequently underwent preprocedural CT-MP assessment before the scheduled PCI procedure for the culprit lesion.

All patients underwent PCI using a 6F system via the radial artery according to the standard technique and latest guidelines. Coronary stent implantation (2nd or 3rd generation drug-eluting stents) was performed with predilatation. The type of stent was selected at the operator's discretion and the strategy was determined by the interventionist. Online quantitative coronary angiography was performed to determine the appropriate stent size for avoiding aggressive stent expansion. Successful PCI was defined as resulting in <20% residual stenosis, thrombolysis in myocardial infarction grade 3 flow, no side branch occlusion or distal embolization, and no PCI-related myocardial infarction.

Coronary CT angiography and the assessments of plaque characteristics

A 320-row multidetector computed tomography (MDCT) system (Aquilion ONE; Canon Medical Systems Corporation, Otawara, Japan) was used for acquisition of MDCT images in accordance with the Society of Cardiovascular Computed Tomography guidelines (9). Coronary artery calcium scores obtained from non-contrast cardiac CT were analyzed using the method described by Agatston *et al.* (10). Quantitative plaque characteristics were analyzed according to the definitions from previous study (11). The 3-D plaque quantification was performed for both the target lesions and target vessels using semi-automated plaque analysis software (QAngioCT Research

Edition version 2.1.9.1, Medis Medical Imaging Systems) with appropriate manual correction (12). Total plaque volume and FFNC volume were selected as clinically relevant parameters from previous study, and plaque quantification in the whole vessel was performed (13).

Epicardial fat volume, epicardial fat attenuation, pericoronary adipose tissue attenuation index (PCATA) and CT-derived cardiac mass analysis

From CCTA images, epicardial fat volume and epicardial fat attenuation were measured using semi-automated analysis software (VirtualPlace, Aze Inc., Otawara, Japan) as previously described (14).

Dedicated workstation (Aquarius iNtuition Edition, version 4.4.13. P3; TeraRecon Inc., Foster City, CA, USA) is used for the analysis of the PCATA. The proximal 40 mm segment of the left anterior-descending artery and left circumflex artery, and proximal 10–50 mm segment of the right coronary artery were traced, as described previously (15). Pericoronary fat attenuation value was determined based on all voxels with CT attenuation between −190 and −30 HU located within a radial distance from the outer vessel wall equal to the diameter of the coronary vessels. Pericoronary fat attenuation was measured by an expert investigator blinded to the clinical data (Sugiyama T).

Quantitative assessment of left ventricular (LV) mass was conducted using the Aquarius iNtuition Workstation Edition version 4.4.13 (TeraRecon Inc.) at the mid-diastole phase, as previously described (16). Two independent investigators (Sugiyama T and Kanaji Y) analyzed the whole target vessel territory cardiac mass and the cardiac mass at risk from the target lesion.

CT-MP assessment

A second-generation 320-row MDCT system (Aquilion ONE; Canon Medical System Corporation) was used for dynamic CT-MP/CCTA examination in accordance with the Society of Cardiovascular Computed Tomography guidelines (9). CT-MP dynamic scans were performed with a tube voltage of 80 kV and tube current of 120 mA at 70–80% of the R-R interval. CCTA and CT-MP protocols have been previously reported (3). Stress dynamic CT-MP with intravenous adenosine triphosphate infusion (0.016 mg/kg/min) was followed by rest dynamic CT-MP. For each dynamic CT-MP examination, 50 mL of contrast medium, followed by a 30-mL saline chaser, was infused at 5 mL/s using a dual-head power injector. A bolus-tracking technique with real-time image reconstruction was used with the region of interest set in the pulmonary artery trunk at a threshold of 100 HU. After a 5-s delay, dynamic CT-MP images were acquired for 25 s using the electrocardiography (ECG) monitoring for prospective triggering with a phase window of only 70–80% of the R-R interval. For dynamic imaging, a tube voltage of 80 kV and a tube current of 120 mA were used.

Rest CCTA imaging was performed as a boost scan during rest dynamic CT-MP, with a tube voltage of 80 kV and tube current of 650 mA [for body mass index (BMI) <22.5 kg/m^2] or 800 mA (for BMI ≥22.5 kg/m^2) at 75% of the R-R interval with 0.5 mm reconstruction. The boost timing was the peak enhancement time of the left main coronary trunk in stress dynamic CT-MP.

Quantitative assessment of MBF using CT-MP imaging was performed using commercially available software Vitrea version 8.10 (Vital Images Inc., Minnesota, USA) as previously reported (17,18). The MBF was calculated using model-independent deconvolution analysis. The time attenuation curve of the ascending aorta was used as the input function. The CT-MBF was evaluated using a 17-segment model. Vessel territory regional and whole-myocardial MBF were assessed.

Statistical analysis

Statistical analyses were performed using SPSS version 25.0 (SPSS, Inc., Chicago, IL, USA). Categorical data are presented as numbers and percentages and were compared using the Chi-squared test. Shapiro-Wilk statistics was used for the assessment of the normality of the distributed values. Continuous data are presented as the mean ± standard deviation for normally distributed variants or as the median [interquartile range (IQR)] for non-normal distribution and were analyzed using the Student's *t*-test and the Mann-Whitney *U* test, respectively. Associations were evaluated by analyzing Pearson's correlation for normally distributed data and Spearman's correlation for non-normally distributed data. Univariate and multivariate logistic regression analyses were performed to predict the occurrence of CMD. The Hosmer-Lemeshow test was used to evaluate the fitness of the models. Receiver operating characteristic (ROC) curve analysis was performed to assess the best cutoff values for predicting CMD. A prediction model for CMD was constructed to determine the incremental discriminatory and reclassification performance of CT plaque analysis findings

Table 1 Baseline characteristics and angiographic data

Patient characteristics	All lesions (n=68)	Non-CMD (n=39)	CMD (n=29)	P value
Age (years old)	69±11	71±10	68±13	0.258
Male/female, n (%)	60 (88.2)/8 (11.8)	34 (87.2)/5 (12.8)	26 (89.7)/3 (10.3)	>0.99
Hemodialysis, n (%)	3 (4.4)	3 (7.7)	0 (0.0)	0.352
Diabetes, n (%)	33 (48.5)	21 (53.8)	12 (41.4)	0.440
Hypertension, n (%)	53 (77.9)	32 (82.1)	21 (72.4)	0.514
Hyperlipidemia, n (%)	37 (54.4)	19 (48.7)	18 (62.1)	0.397
Smoking, n (%)	19 (27.9)	10 (25.6)	9 (31.0)	0.828
Prior myocardial infarction, n (%)	14 (20.6)	5 (12.8)	9 (31.0)	0.125
Ejection fraction (%)	63±10	63±10	63±10	0.783
Lesion location (RCA/LAD/LCx), n (%)	13 (19.1)/48 (70.6)/7 (10.3)	7 (17.9)/29 (74.4)/3 (7.7)	6 (20.7)/19 (65.5)/4 (13.8)	0.653
Pre PCI				
Diameter stenosis	58.93±12.67	58.01±13.06	60.15±12.25	0.495
Minimal lumen diameter	1.04±0.35	1.00±0.33	1.10±0.36	0.259
Lesion length	14.66 (10.27–21.93)	16.92 (10.81–24.05)	13.60 (10.17–19.04)	0.239
Reference diameter	2.47 (2.20–2.81)	2.39 (2.16–2.74)	2.61 (2.33–3.19)	0.038
Post PCI				
Diameter stenosis	18.36±6.82	16.90±5.52	20.32±7.93	0.040
Minimal lumen diameter	2.68±0.44	2.67±0.37	2.69±0.54	0.876
Lesion length	17.56 (11.37–24.17)	20.89 (12.17–24.91)	14.46 (10.82–21.44)	0.261
Reference diameter	3.23 (3.02–3.56)	3.27 (2.88–3.54)	3.19 (3.07–3.69)	0.442

Continuous data are expressed as the mean ± standard deviation for normally distributed variants or as the median (interquartile range) for non-normal distribution and were analyzed using the Student's *t*-test and the Mann-Whitney *U* test, respectively. CMD, coronary microvascular dysfunction; RCA, right coronary artery; LAD, left anterior-descending artery; LCx, left circumflex artery; PCI, percutaneous coronary intervention.

and CT-MP indices using relative integrated discrimination improvement (IDI) and category-free net reclassification index (NRI). Statistical significance was set at P<0.05.

Results

Baseline characteristics and angiographic and physiological findings

Tables 1,*2* summarize the baseline characteristics and angiographic and physiological data of 68 patients in two groups divided by IMR <25 or IMR ≥25. Thirty-nine lesions (57.4%) were non-CMD and 29 (42.6%) were CMD. Lesion distribution showed 13 lesions (19.1%) in the right coronary artery, 48 (70.6%) in the left anterior-descending artery, and 7 (10.3%) in the left circumflex artery. In lesions with CMD, the reference diameter was larger compared to those without CMD [2.61 (IQR, 2.33–3.19) *vs.* 2.39 (IQR, 2.16–2.74), P=0.038].

In CT-MP-derived regional analysis, rest MBF of lesions CMD was comparable between the two groups with and without CMD [0.80 (IQR, 0.59–0.95) and 0.90 (IQR, 0.69–1.12) mL/min/g, P=0.199). The hyperemic-MBF of lesions without CMD was significantly higher than those with CMD [2.31 (IQR, 1.67–3.34) and 1.68 (IQR, 0.84–2.44) mL/min/g, P=0.015]. The prevalence of $CFR_{CT\text{-}MP}$ <2.0 was significantly higher in lesions with CMD than in those without CMD (62.1% *vs.* 28.2%, P=0.011).

The median estimated radiation dose was 19.8 (18.8–

Table 2 Perfusion CT and wire-derived physiological data

Physiological indices	All lesions (n=68)	Non-CMD (n=39)	CMD (n=29)	P value
Perfusion CT indices in target vessel area				
CFR_{CT-MP}	2.19 (1.44–3.37)	2.63 (1.83–3.36)	1.79 (1.14–3.36)	0.076
CFR_{CT-MP} <2.0, n (%)	29 (42.6)	11 (28.2)	18 (62.1)	0.011
Rest MBF (mL/min/g)	0.83 (0.64–1.03)	0.90 (0.69–1.12)	0.80 (0.59–0.95)	0.199
Hyperemic MBF (mL/min/g)	2.14 (1.30–2.92)	2.31 (1.67–3.34)	1.68 (0.84–2.44)	0.015
Perfusion CT indices in whole myocardium				
CFR_{CT-MP}	2.49 (1.72–3.48)	2.61 (2.06–3.47)	1.80 (1.14–3.52)	0.095
CFR_{CT-MP} <2.0, n (%)	25 (36.8)	10 (25.6)	15 (51.7)	0.051
Rest MBF (mL/min/g)	0.82 (0.64–1.10)	0.89 (0.68–1.12)	0.75 (0.64–1.06)	0.286
Hyperemic MBF (mL/min/g)	2.25 (1.41–2.99)	2.32 (1.78–3.50)	2.04 (0.81–2.45)	0.022
Wire-derived physiological indices				
Pre-PCI CFR_{wire}	1.71 (1.24–2.88)	1.88 (1.26–3.09)	1.63 (1.17–2.73)	0.277
Pre-PCI FFR	0.68 (0.59–0.74)	0.67 (0.60–0.72)	0.68 (0.59–0.75)	0.589
Pre-PCI IMR Pw cor	22.6 (15.1–34.5)	17.9 (10.8–19.4)	35.7 (30.6–45.1)	<0.001
Post-PCI CFR_{wire}	2.66 (1.72–4.32)	2.45 (1.65–3.61)	2.86 (1.87–5.05)	0.111
Post-PCI FFR	0.85 (0.80–0.92)	0.83 (0.80–0.90)	0.89 (0.82–0.94)	0.037
Post-PCI IMR	20.5 (13.8–29.8)	14.0 (10.9–20.8)	29.3 (21.6–37.7)	<0.001

Continuous data are expressed as the median (interquartile range) distribution and were analyzed using the Mann-Whitney *U* test for non-normal distribution. CT, computed tomography; CMD, coronary microvascular dysfunction; CFR, coronary flow reserve; CT-MP, computed tomography myocardial perfusion; MBF, myocardial blood flow; PCI, percutaneous coronary intervention; FFR, fractional flow reserve; IMR, index of microcirculatory resistance; Pw, coronary wedge pressure; cor, correction.

22.8) mSv for CT studies.

CT plaque analysis

Table 3 summarizes the results of CT plaque analysis. On per-plaque analysis, FFNC volume was significantly greater in lesions with CMD than in those without [31.8 (IQR, 19.0–48.9) and 25.1 (IQR, 17.2–32.1) mm^3, P=0.045]. Epicardial fat volume was significantly higher in lesions with CMD than in those without [166 (IQR, 124–215) and 126 (IQR, 97–172) mm^3, P=0.023]. Epicardial fat attenuation was not significantly different between lesions with and without CMD [–80.03 (IQR, –83.79 to –76.24) and –83.08 (IQR, –84.82 to –78.62) HU, P=0.333].

Pericoronary fat attenuation index

Table 4 shows the pericoronary fat attenuation index in lesions with and without CMD. There were no significant differences in the PCATA of the PCI target vessel, right coronary artery, and left anterior-descending artery and the mean value of the three vessels between non-CMD and CMD territories.

Determinants of CMD

Regional CFR_{CT-MP} <2.0, regional hyperemic MBF, whole cardiac CFR_{CT-MP} <2.0, whole cardiac stress MBF, FFNC volume, and epicardial fat volume were significant predictors of CMD on univariate logistic regression analysis. As for the significant predictors in univariate analysis, regional CFR_{CT-MP} <2.0 and regional hyperemic MBF were selected as regional CT-derived flow variables, and FFNC volume and epicardial fat volume were selected as morphological characteristics in coronary plaques and the epicardium.

For the multivariable logistic regression analysis, four models using significant predictors in the univariate analyses

Table 3 CT plaque analysis

CT plaque analysis	All lesions (n=68)	Non-CMD (n=39)	CMD (n=29)	P value
Per-vessel analysis				
Vessel volume (mm^3)	845.5 (659.1–1,071.2)	859.1 (606.4–1,104.9)	837.2 (734.8–1,048.2)	0.692
Plaque volume (mm^3)	443.6 (281.9–625.4)	488.5 (278.1–700.0)	439.6 (337.5–497.3)	0.506
Fibrous volume (mm^3)	240.5 (198.3–305.7)	218.3 (187.1–296.8)	244.4 (211.5–317.9)	0.402
FFNC volume (mm^3)	41.6 (33.4–62.5)	42.02 (33.8–56.4)	40.7 (31.4–69.6)	0.673
Dense calcium volume (mm^3)	132.1 (27.0–269.5)	173.9 (30.8–312.2)	84.7 (8.9–186.5)	0.089
Plaque analysis				
Vessel volume (mm^3)	342.5 (242.5–513.2)	322.5 (220.4–479.1)	364.0 (291.4–579.8)	0.207
Plaque volume (mm^3)	200.0 (133.2–332.3)	192.1 (114.2–323.9)	220.7 (144.7–351.0)	0.579
Fibrous volume (mm^3)	111.5 (67.6–152.8)	104.7 (62.2–133.1)	116.7 (92.0–160.7)	0.217
FFNC volume (mm^3)	25.5 (18.1–37.8)	25.1 (17.2–32.1)	31.8 (19.0–48.9)	0.045
Dense calcium volume (mm^3)	48.4 (4.5–160.0)	50.5 (8.7–171.1)	47.4 (2.6–145.0)	0.468
Plaque burden mean (%)	81.0 (71.0–88.2)	80.5 (66.8–88.2)	81.5 (71.5–87.6)	0.777
Epicardial fat volume (mm^3)	158 [108–195]	126 [97–172]	166 [124–215]	0.023
Epicardial fat attenuation (HU)	−80.60 (−84.70, −76.78)	−80.03 (−83.79, −76.24)	−83.08 (−84.82, −78.62)	0.333
Agatston score	644 (233–1,499)	678 (276–2,110)	610 (134–1,157)	0.271
Subtended mass of target vessel (mm^3)	51.1 (40.2–71.5)	51.4 (40.1–76.4)	50.4 (40.7–68.4)	0.775
Subtended mass of target lesion (mm^3)	47.6 (37.3–60.2)	50.8 (37.9–59.0)	45.4 (34.3–60.2)	0.556

Continuous data are expressed as the median (interquartile range)/[interquartile range] distribution and were analyzed using the Mann-Whitney *U* test for non-normal distribution. CT, computed tomography; CMD, coronary microvascular dysfunction; FFNC, fibrofatty and necrotic component.

Table 4 CT plaque analysis-peri coronary fat

PCATA analysis	All lesions (n=68)	Non-CMD (n=39)	CMD (n=29)	P value
PCATA of PCI target vessel	−75.66±10.10	−76.79±10.86	−74.14±8.94	0.288
PCATA of RCA	−77.68±11.82	−77.76±12.21	−77.56±11.47	0.946
PCATA of LAD	−75.40±9.39	−75.27±10.72	−75.58±7.41	0.893
PCATA of three vessels	−75.66±10.10	−76.79±10.86	−74.14±8.94	0.288

Continuous data are expressed as the mean ± standard and were analyzed using the Student's *t*-test deviation for normally distributed variants. CT, computed tomography; PCATA, pericoronary adipose tissue attenuation index; CMD, coronary microvascular dysfunction; PCI, percutaneous coronary intervention; RCA, right coronary artery; LAD, left anterior-descending artery.

were constructed. The Hosmer-Lemeshow test indicated that the model using a combination of regional hyperemic MBF and FFNC volume showed the best fit for predicting CMD (*Table 5*). ROC analysis revealed the best cut-off values of these two variables for predicting coexisting CMD were regional hyperemic MBF <2.59 mL/min/g [area under the curve (AUC): 0.674; 95% confidence interval (CI): 0.545–0.804] and FFNC volume >31.68 (AUC: 0.644; 95% CI: 0.507–0.780), respectively.

The addition of FFNC- and CT-MP-derived hyperemic MBF to regional $CFR_{CT\text{-}MP}$ and epicardial fat volume significantly improved the ability to predict the presence of

Table 5 Logistic regression analysis predicting CMD

Predictors of CMD	Univariable analysis			Multivariable analysis 1			Multivariable analysis 2			Multivariable analysis 3			Multivariable analysis 4		
	Odds ratio	95% CI	P value	Odds ratio	95% CI	P value	Odds ratio	95% CI	P value	Odds ratio	95% CI	P value	Odds ratio	95% CI	P value
Wire-derived physiological indices															
Pre-PCI CFR_{wire}	0.748	0.474–1.180	0.210	–	–	–	–	–	–	–	–	–	–	–	–
Pre-PCI FFR	4.53	0.036–567.0	0.540	–	–	–	–	–	–	–	–	–	–	–	–
Regional $CFR_{CT\text{-}MP}$	0.734	0.506–1.060	0.103	–	–	–	–	–	–	–	–	–	–	–	–
Regional $CFR_{CT\text{-}MP}$ <2.0	4.170	1.500–11.600	0.006	–	–	–	4.380	1.450–13.200	0.009	–	–	–	3.820	1.320–11.100	0.014
Regional rest MBF (mL/min/g)	0.690	0.256–1.860	0.464	–	–	–	–	–	–	–	–	–	–	–	–
Regional hyperemic MBF (mL/min/g)	0.565	0.350–0.911	0.019	0.583	0.355–0.958	0.033	–	–	–	0.573	0.3510–0.934	0.026	–	–	–
Whole cardiac $CFR_{CT\text{-}MP}$	0.729	0.298–1.070	0.102	–	–	–	–	–	–	–	–	–	–	–	–
Whole cardiac $CFR_{CT\text{-}MP}$ <2.0	3.110	1.120–8.650	0.030	–	–	–	–	–	–	–	–	–	–	–	–
Whole cardiac rest MBF (mL/min/g)	0.753	0.264–2.150	0.595	–	–	–	–	–	–	–	–	–	–	–	–
Whole cardiac hyperemic MBF (mL/min/g)	0.577	0.357–0.9311	0.024	–	–	–	–	–	–	–	–	–	–	–	–
FFNC volume (mm^3)	1.040	1.010–1.070	0.011	1.04	1.01–1.07	0.018	1.040	1.010–1.080	0.012	–	–	–	–	–	–
Epicardial fat volume (mm^3)	1.010	1.000–1.020	0.018	–	–	–	–	–	–	1.010	1.000–1.020	0.025	1.010	1.000–1.020	0.037
Hosmer-Lemeshow test (P value)	–	–	–		0.843			0.112			0.014			0.651	

CMD, coronary microvascular dysfunction; CI, confidence interval; PCI, percutaneous coronary intervention; CFR, coronary flow reserve; FFR, fractional flow reserve; CT-MP, computed tomography myocardial perfusion; MBF, myocardial blood flow; FFNC, fibrofatty and necrotic component.

Table 6 Prediction model for CMD

Prediction model	C-statistic	P value	IDI	P value	NRI	P value
Clinical model 1	0.737	–	Reference		Reference	
Clinical model 2	0.781	0.226	0.077	0.029	0.522	0.025
Clinical model 3	0.783	0.177	0.093	0.015	0.368	0.124
Clinical model 2	0.781	–	Reference		Reference	
Clinical model 3	0.783	0.849	0.016	0.325	0.508	0.030

Clinical model 1 (regional CFR_{CT-MP} <2.0 + epicardial fat volume). Clinical model 2 (regional CFR_{CT-MP} <2.0 + epicardial fat volume + FFNC volume). Clinical model 3 (regional CFR_{CT-MP} <2.0 + epicardial fat volume + FFNC volume + regional hyperemic MBF). CMD, coronary microvascular dysfunction; IDI, integrated discrimination improvement; NRI, net reclassification index; CFR, coronary flow reserve; CT-MP, computed tomography myocardial perfusion; FFNC, fibrofatty and necrotic core component; MBF, myocardial blood flow.

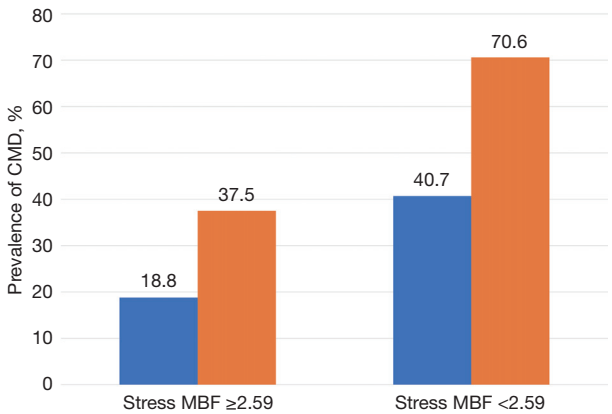

Figure 2 Prevalence of CMD. The total cohort was divided into four groups according to the best cutoff values for regional hyperemic MBF and FFNC volume, and the prevalence of CMD in the four groups was significantly different. Blue bar shows FFNC ≤31.68 mm^3, and orange bar shows FFNC >31.68 mm^3. MBF, myocardial blood flow; CMD, coronary microvascular dysfunction; FFNC, fibrofatty and necrotic core components.

CMD (*Table 6*).

When the total cohort was divided into four groups according to the best cutoff values for regional hyperemic MBF and NNFC volume, the prevalence of CMD in the four groups was significantly different (P=0.026; *Figure 2*).

Discussion

This study aimed to clarify the diagnostic value of CT-MP-derived coronary flow indices and CCTA-based plaque analysis for detecting lesions with coexisting microvascular dysfunction in patients with *de novo* functionally stenotic lesions. The major findings were (I) the prevalence of CMD was 42.6%; (II) hyperemic MBF and FFNC volume were both significant predictors of CMD; (III) reference diameter was larger in lesions with CMD compared to those without CMD; (IV) CT-MP-derived hyperemic MBF had incremental diagnostic efficacy in addition to FFNC. In the lesions with hyperemic MBF <2.59 and FFNC >31.68, CMD accounted up to 70.6% of all target vessel territories, compared with 18.8% with neither of these two factors.

To the best of our knowledge, this is the first study to investigate the diagnostic performance of CT-MP findings in vessel territories with coexisting microvascular dysfunction in patients undergoing FFR-guided PCI. The present study indicated that 42.6% of territories with functionally significant stenotic lesions exhibited coexistence of CMD. Our results also indicate that CCTA-defined plaque characteristics are associated with microvascular dysfunction. Our report is in line with a review by Crea *et al.*, which reported a significant association between the risk factors for CMD and atherosclerosis (4).

Clinical implications

CT-MP has been reported to be a useful modality for identifying or ruling out hemodynamically significant coronary lesions (19). However, the diagnostic efficacy of CT-MP for detecting CMD and its clinical implications in patients with coexisting CMD with functionally significant lesions undergoing PCI remain to be determined. Our results suggest that CT-MP can help determine the presence of CMD in PCI target territories. Further studies with larger sample sizes are needed to test our hypothesis-generating results and evaluate the prognostic value of pre-PCI CMD in target territories after PCI.

Limitation

This study had several important limitations. The present study included only 68 lesions in the final analysis. The study design, including its single-center, non-randomized, observational nature, could only provide hypothesis-generating results. All the patients included in the present study had functionally significant lesions. Lesions with CMD but without epicardial significance were not assessed. CMD was assessed using only IMR; the difference between diffuse coronary artery disease and microvascular disease was not assessed. Patients with severe renal dysfunction were excluded because of the contrast used for CT-MP. The rigorous exclusion criteria and CT protocols limited the number of study patients and may have resulted in a certain level of selection bias. In particular, 88.2% of the patients were male, which may limit the generalizability of the present study's results.

A control group of patients without chest pain or evidence of atherosclerosis was not included in the present study. Therefore, the prevalence of CMD in asymptomatic patients without significant stenosis could not be assessed based on the results of the present study.

However, the strength of the present study is that all data were obtained using the same CT modality (a 320 detector raw CT system).

Conclusions

Coexisting CMD is not uncommon in territories with functionally significant epicardial lesions in patients that undergo PCI. Absolute coronary flow assessment using CT-MP and plaque analysis using CCTA may help detect coexisting subtended microvascular dysfunction in patients with CCS and functionally significant epicardial coronary lesions. Further studies are needed to validate our hypothesis-generating results and assess the clinical significance of coexisting CMD in patients undergoing PCI.

Acknowledgments

The authors thank all physicians, nurses, radiographers, other heart team members, and patients who were involved in this study. And this study was presented at the European Society of Cardiology Congress 2022.

Funding: None.

Footnote

Reporting Checklist: The authors have completed the STROBE reporting checklist. Available at https://qims.amegroups.com/article/view/10.21037/qims-23-618/rc

Conflicts of Interest: All authors have completed the ICMJE uniform disclosure form (available at https://qims.amegroups.com/article/view/10.21037/qims-23-618/coif). The authors have no conflicts of interest to declare.

Ethical Statement: The authors are accountable for all aspects of the work and ensure that questions related to the accuracy or integrity of any part of the work are appropriately investigated and resolved. The study was approved by the Institutional Ethics Committee of Tsuchiura Kyodo General Hospital (reference #808/Tsuchiura; March 22, 2019) and conducted in compliance with the tenets of the Declaration of Helsinki (as revised in 2013) for investigations with human participants. All patients provided written informed consent for the study and future data use for retrospective analyses.

References

1. George RT, Arbab-Zadeh A, Miller JM, Kitagawa K, Chang HJ, Bluemke DA, Becker L, Yousuf O, Texter J, Lardo AC, Lima JA. Adenosine stress 64- and 256-row detector computed tomography angiography and perfusion imaging: a pilot study evaluating the transmural extent of perfusion abnormalities to predict atherosclerosis causing myocardial ischemia. Circ Cardiovasc Imaging 2009;2:174-82.
2. Rochitte CE, George RT, Chen MY, Arbab-Zadeh A, Dewey M, Miller JM, et al. Computed tomography angiography and perfusion to assess coronary artery

stenosis causing perfusion defects by single photon emission computed tomography: the CORE320 study. Eur Heart J 2014;35:1120-30.
3. Kikuchi Y, Oyama-Manabe N, Naya M, Manabe O, Tomiyama Y, Sasaki T, Katoh C, Kudo K, Tamaki N, Shirato H. Quantification of myocardial blood flow using dynamic 320-row multi-detector CT as compared with ^{15}O-H_2O PET. Eur Radiol 2014;24:1547-56.
4. Crea F, Camici PG, Bairey Merz CN. Coronary microvascular dysfunction: an update. Eur Heart J 2014;35:1101-11.
5. Hu X, Zhang J, Lee JM, Chen Z, Hwang D, Park J, Shin ES, Nam CW, Doh JH, Chen S, Yang J, Tanaka N, Kuramitsu S, Matsuo H, Takashima H, Akasaka T, Koo BK, Wang J. Prognostic impact of diabetes mellitus and index of microcirculatory resistance in patients undergoing fractional flow reserve-guided revascularization. Int J Cardiol 2020;307:171-5.
6. Taqueti VR, Hachamovitch R, Murthy VL, Naya M, Foster CR, Hainer J, Dorbala S, Blankstein R, Di Carli MF. Global coronary flow reserve is associated with adverse cardiovascular events independently of luminal angiographic severity and modifies the effect of early revascularization. Circulation 2015;131:19-27.
7. Hoshino M, Yang S, Sugiyama T, Zhang J, Kanaji Y, Hamaya R, et al. Characteristic findings of microvascular dysfunction on coronary computed tomography angiography in patients with intermediate coronary stenosis. Eur Radiol 2021;31:9198-210.
8. Aarnoudse W, van den Berg P, van de Vosse F, Geven M, Rutten M, Van Turnhout M, Fearon W, de Bruyne B, Pijls N. Myocardial resistance assessed by guidewire-based pressure-temperature measurement: in vitro validation. Catheter Cardiovasc Interv 2004;62:56-63.
9. Abbara S, Blanke P, Maroules CD, Cheezum M, Choi AD, Han BK, Marwan M, Naoum C, Norgaard BL, Rubinshtein R, Schoenhagen P, Villines T, Leipsic J. SCCT guidelines for the performance and acquisition of coronary computed tomographic angiography: A report of the society of Cardiovascular Computed Tomography Guidelines Committee: Endorsed by the North American Society for Cardiovascular Imaging (NASCI). J Cardiovasc Comput Tomogr 2016;10:435-49.
10. Agatston AS, Janowitz WR, Hildner FJ, Zusmer NR, Viamonte M Jr, Detrano R. Quantification of coronary artery calcium using ultrafast computed tomography. J Am Coll Cardiol 1990;15:827-32.
11. Motoyama S, Ito H, Sarai M, Kondo T, Kawai H, Nagahara Y, Harigaya H, Kan S, Anno H, Takahashi H, Naruse H, Ishii J, Hecht H, Shaw LJ, Ozaki Y, Narula J. Plaque Characterization by Coronary Computed Tomography Angiography and the Likelihood of Acute Coronary Events in Mid-Term Follow-Up. J Am Coll Cardiol 2015;66:337-46.
12. Park HB, Lee BK, Shin S, Heo R, Arsanjani R, Kitslaar PH, Broersen A, Dijkstra J, Ahn SG, Min JK, Chang HJ, Hong MK, Jang Y, Chung N. Clinical Feasibility of 3D Automated Coronary Atherosclerotic Plaque Quantification Algorithm on Coronary Computed Tomography Angiography: Comparison with Intravascular Ultrasound. Eur Radiol 2015;25:3073-83.
13. Nakazato R, Shalev A, Doh JH, Koo BK, Gransar H, Gomez MJ, Leipsic J, Park HB, Berman DS, Min JK. Aggregate plaque volume by coronary computed tomography angiography is superior and incremental to luminal narrowing for diagnosis of ischemic lesions of intermediate stenosis severity. J Am Coll Cardiol 2013;62:460-7.
14. Oda S, Utsunomiya D, Funama Y, Yuki H, Kidoh M, Nakaura T, Takaoka H, Matsumura M, Katahira K, Noda K, Oshima S, Tokuyasu S, Yamashita Y. Effect of iterative reconstruction on variability and reproducibility of epicardial fat volume quantification by cardiac CT. J Cardiovasc Comput Tomogr 2016;10:150-5.
15. Oikonomou EK, Marwan M, Desai MY, Mancio J, Alashi A, Hutt Centeno E, et al. Non-invasive detection of coronary inflammation using computed tomography and prediction of residual cardiovascular risk (the CRISP CT study): a post-hoc analysis of prospective outcome data. Lancet 2018;392:929-39.
16. Klein R, Ametepe ES, Yam Y, Dwivedi G, Chow BJ. Cardiac CT assessment of left ventricular mass in mid-diastasis and its prognostic value. Eur Heart J Cardiovasc Imaging 2017;18:95-102.
17. Tanabe Y, Kido T, Uetani T, Kurata A, Kono T, Ogimoto A, Miyagawa M, Soma T, Murase K, Iwaki H, Mochizuki T. Differentiation of myocardial ischemia and infarction assessed by dynamic computed tomography perfusion imaging and comparison with cardiac magnetic resonance and single-photon emission computed tomography. Eur Radiol 2016;26:3790-801.
18. Kono T, Uetani T, Inoue K, Nagai T, Nishimura K,

Suzuki J, Tanabe Y, Kido T, Kurata A, Mochizuki T, Ogimoto A, Okura T, Higaki J, Yamaguchi O, Ikeda S. Diagnostic accuracy of stress myocardial computed tomography perfusion imaging to detect myocardial ischemia: a comparison with coronary flow velocity reserve derived from transthoracic Doppler echocardiography. J Cardiol 2020;76:251-8.

19. Obara M, Naya M, Oyama-Manabe N, Aikawa T, Tomiyama Y, Sasaki T, Kikuchi Y, Manabe O, Katoh C, Tamaki N, Tsutsui H. Diagnostic value of quantitative coronary flow reserve and myocardial blood flow estimated by dynamic 320 MDCT scanning in patients with obstructive coronary artery disease. Medicine (Baltimore) 2018;97:e11354.

Cite this article as: Hada M, Hoshino M, Sugiyama T, Kanaji Y, Usui E, Hanyu Y, Nagamine T, Nogami K, Ueno H, Matsuda K, Sakamoto T, Yonetsu T, Sasano T, Kakuta T. Diagnostic value of computed tomography myocardial perfusion imaging to detect coexisting microvascular dysfunction in patients with obstructive epicardial coronary artery disease. Quant Imaging Med Surg 2023;13(12):8423-8434. doi: 10.21037/qims-23-618

